Received: September 4, 2023. Revised: October 16, 2023.

International Journal of
Intelligent Engineering & Systems

http://www.inass.org/

The Powerful Activity for FBMC-OQAM Wireless Communication System Relies on Slantlet Transform

Raad Farhood Chisab[1]*

[1]*Technical Institute Kut, Middle Technical University, Baghdad, Iraq*
* Corresponding author's Email: raadfarhood@yahoo.com

Abstract: There are many candidate waveforms for the next-era communication system. Filter bank multi-carrier (FBMC) This system depends on offset quadrature amplitude modulation (OQAM) is one of them. Compared to OFDM, it can offer faster data rates and improved spectrum efficiency. The OFDM has a few disadvantages which as a high PAPR resulting in the requirement for high-power amplifiers. So, to overcome this problem, the FBMC system with OQAM is used. In this manuscript, a proposed method was designed using the modified technique through the slantlet transform (ST) to raise the activity for the system. This scheme is suitable for providing lower losses, higher data rates, and for better spectral efficiency. a proposed method that uses the ST gives a modified performance than the fast fourier transform (FFT). Many parameters were applied to test the activity of the system such As Power spectral density, prototype filters, signal power, velocity, carrier frequency, modulation order, power delay profile, channel doppler model, overlap factor, and efficiency. In all these parameters it can be noticed that the proposed system based on ST has overcome the other systems and gives higher performance.

Keywords: FBMC, OQAM, Slantlet transform, BER, PSD.

1. Introduction

Time-frequency localization refers to the ability to precisely determine both the temporal and frequency characteristics of a signal. In various fields such as signal processing, communications, and physics, understanding the behavior of a signal in the frequency and time fields is crucial for extracting meaningful information and making accurate analyses. Symbols are conveyed across a rectangular time-frequency grid in such a multicarrier system [1-3]. Be aware that the form in frequency and, therefore, in time is determined by the subcarrier spacing. Low latency transmissions are made possible by large subcarrier spacing, while bandwidth efficiency is increased by tiny subcarrier spacing. Additionally, varied subcarrier spacings enable the transmission system to be matched to certain channel circumstances [4-6]. High subcarrier spacing should be used by a user traveling at high speeds. On the other hand, a short subcarrier spacing is preferable if the multi-path postponement spread is the restrictive factor [7-9]. The 5G of mobile structures uses adaptable subcarrier spacings, as seen in Fig. 1. Future wireless systems can use FBMC thanks to two crucial findings. To effectively accommodate a range of user needs and channel characteristics, flexible time-frequency allocation is initially required. Second, low channel delay spread, mainly when using high carrier frequencies MIMO beam forming inside compact heterogeneous networks [10-12]. The two main problems in wireless communication are: when transmitting the signal how can get the transmitted signal to the receiving end without error which means the bit error rate BER. The second problem in wireless communication is the out-of-band OOB emission. That means how to limit the signal transmitted in a limited band of frequency. when controlling this problem leads to reduced power consumption and consequently the long life of battery used in equipment. To solve these two problems many systems were invented to reduce BER and OOB. These systems such as: WOLA, UFMC,

Table 1. The variables used in the simulation

Variables symbol	The meaning of variable
$s(t)$	The total transmitted signal
$x_{l,k}$	Signal in subcarrier location l and location of time k
$g_{l,k}(t)$	The basis pulse
P_{TX}	a shifted form of the filter
$\theta_{l,k}$	phase shifting
σ_t	Time localization
σ_f	Frequency localization
$P(f)$	the Fourier transform of p(t)
$\bar{t}$	the mean of time
$\bar{f}$	the mean of frequency
R{.}	the real portions of a quantity character
J{.}	the imaginary portions of a quantity character
$H_n(\cdot)$	Hermite polynomials
$a_0, a_4, a_8, a_{12}, a_{16}, a_{20}.$	the coefficients of *P(t)* filter
N	The number of Slantlet transform basis
K	The number of zero moments
$g_i(n),\ h_i(n)\ , f_i(n)$	The filter bank in the Slantlet transform
$m, s_1, t_1, s_0, t_0.$	The variable for calculating $a_{0,0}. a_{0,1}. a_{1,0}\ .\ a_{1,1}.$
$a_{0,0}. a_{0,1}. a_{1,0}\ .\ a_{1,1}.$	The variable for calculating $g_i(n)$
u, v	The variable for calculating $b_{0,0}. b_{0,1}. b_{1,0}\ .\ b_{1,1}.$
$b_{0,0}. b_{0,1}. b_{1,0}\ .\ b_{1,1}.$	The variable for calculating $h_i(n)$
q	The variable for calculating $c_{0,0}. c_{0,1}. c_{1,0}\ .\ c_{1,1}.$
$c_{0,0}. c_{0,1}. c_{1,0}\ .\ c_{1,1}.$	The variable for calculating $f_i(n)$

OFDM, FOFDM, FBMC (which will be taken in detail in this paper). During the section on (results and discussion), it can be shown that the FBMC gives the lower OOB with minimum BER among these other systems. In this paper, the modification on FBMC was done to make the system more beneficial and reduce BER and OOB by replacing the fast fourier transform FFT in the sending and receiving end with the slantlet transform ST. This modification in the system makes it the best system between all the previous systems as shown in the figures within the results and discussion part of this paper and this is the aim of this paper.

The stronger points for the proposed method were that it gives a lower bit error rate, lower OOB, lower power dissipated, high stability against the types of noise, best power spectral density, high signal-to-interference ratio, and high efficiency. All these facilities make this method superior to other methods. The entire of these points of power will be proved via the figures that will be explained in the results and discussion part.

The organization of this manuscript as shown: section two takes into account the multicarrier modulation and how to transfer the signals orthogonally with the modulation of multicarrier. Section 3 takes into account the proposed method in all details. Beginning from the description of parts of the system in sending and receiving end. The parts of the system which are FBMC and OQAM also taking in details. Also, the core of the system which is the Slantlet transform was mentioned in details in this part. Section 4 demonstrate the effects of the effected parameters on the activity of the system and compares it with another system. These parameters are channel velocity, channel doppler model, channel carrier frequency, OQAM modulation order, prototype filter, number of subcarriers, number of symbols in time, and subcarrier spacing. Section 5 in which conclude that the system according to activity and figures that it is the best system when compared with other system that taking in this paper. Finally, the references that is used was recorded.

2. Multicarrier modulation

In the field of wireless communication, multicarrier modulation techniques have garnered a lot of attention. This is largely attributable to their ability to efficiently combat frequency-selective fading's negative impacts, improve spectral efficiency, and ease the transmission of large amounts of data. Among these methods, filter bank multicarrier (FBMC) has emerged as a modulation strategy that is especially promising, drawing interest for possible benefits over the widely used orthogonal frequency division multiplexing (OFDM) method. The main goal of this study review is to provide a thorough overview of several multicarrier modulation methods, with a focus on FBMC in particular. We will briefly outline their core ideas, advantages, difficulties, and most recent advancements in this dynamic sector in this study.

In order to explain all the variables used in the simulation within this paper, Table 1. explain all these variables with their meanings.

Additionally, the channel estimate procedure is often made simpler, making adaptive modulation and coding approaches viable [13,14]. The mathematical formula for the transmitted signal in time-domain of system is.

$$s(t) = \sum_{k=1}^{K} \sum_{l=1}^{L} g_{l,k}(t) x_{l,k}\ . \qquad (1)$$

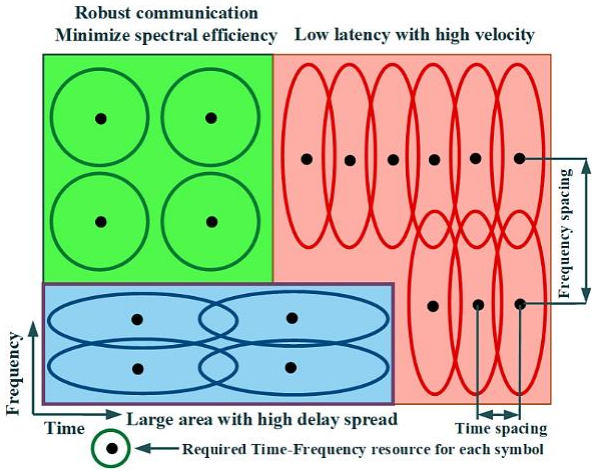

Figure. 1 Wireless systems with stretchy frequency-time resources

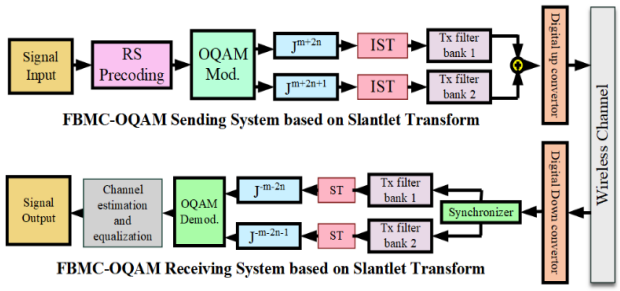

Figure. 2 the proposed system of ST-FBMC-OQAM

Here $x_{l,k}$ represents the signal transmitted in subcarrier location l and location of time k. this is select via a character X. The basis pulse $g_{l,k}(t)$ was definite as.

$$g_{l,k}(t) = P_{TX}(t - KT)e^{j2\pi lF(t-KT)}e^{j\theta_{l,k}} \quad (2)$$

It is basically a shifted form of the filter P_{TX} meaning the space of time and the space of frequency. The selection of the phase shifting, $\theta_{l,k}$ will be pertinent advanced in the situation of a multicarrier scheme.

The balian-low formula, that contends that it is theoretically impossible for the subsequent four desirable attributes to be satisfied simultaneously, indicates that there are basic restrictions on multicarrier systems [15].

1. density of the symbol was Maximum. $TF = 1$.
2. localization of the Time.

$$\sigma_t = \sqrt{\int_{-\infty}^{\infty}(t - \bar{t})^2|p(t)|^2dt} < \infty \quad (3)$$

3. Frequency localization.

$$\sigma_f = \sqrt{\int_{-\infty}^{\infty}(f - \bar{f})^2|p(f)|^2df} < \infty \quad (4)$$

Where δ signifying the Kronecker delta role. the pulse $P(f) = \int_{-\infty}^{\infty} p(t)e^{-j2\pi ftdt}$ signifies the FT of p(t). whereas $\bar{t} = \int_{-\infty}^{\infty} t\,|p(t)|^2\,dt$ equivalent to the mean time. $\bar{f} = \int_{-\infty}^{\infty} f\,|p(f)|^2\,df$ the mean freq. of the pulse. Also, by take up that p(t) was regularized to reservation unit power. The localization quantity could be occupied as standard deviation with $|p(t)|^2$ and $|p(f)|^2$. representative the function of the density probability [16].

3. The proposed FBMC-OQAM based on the slantlet transform (ST)

In this part the proposed system will be described in details. In this system the FFT will be substituted by the ST. this is to get a best result according to the modified specification of ST and also change the characteristics of other block to get the best results. the slantlet transform has a specification that make the system more resistance to the noise and more localization in time and frequency. Therfore, when run this system and according to the output signal it can be shown that the bit error rate become more less than the system based on the traditional system on FFT. It can be seen from Fig. 2 which representes the block map of the projected scheme rely on the slantlet transform in which the block of FFT is replaced by the block of ST. that means the system with more relaibilty, more noise reduction, more power spectral density (PSD), and so on.

In order to prove the activity of proposed system many factors must be taken which give the indication of improvement of the system. These factors are: BER. PSD. Signal Power SP. SNR. SIR. and efficiency. In order to understand the details for system. the parts of the proposed scheme will be described in details and with the aid of figures and equations.

The FBMC is the system's central component. This type of modulation uses multiple carriers. It is an improvement on OFDM and seeks to address some of the problems [17]. Although more signal processing is required as a result. Within a given radio spectrum bandwidth, FBMC is able to provide higher data rates because it uses the available channel capacity much more effectively [18]. It is more efficient in terms of spectrum use. In order to address some of the issues with OFDM, filter bank multicarrier was developed. OFDM has evolved into filter bank multicarrier. employing banks of filters

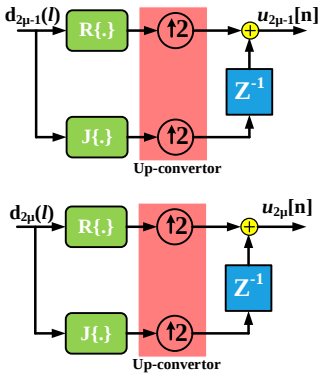

Figure. 3 Pre-processing OQAM for two nearby subchannels

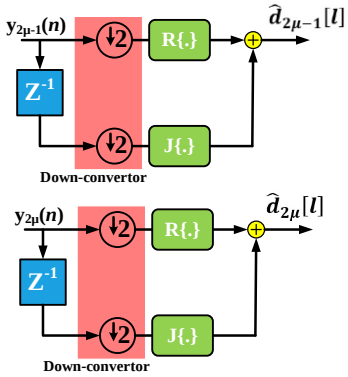

Figure. 4 processing of two neighboring OQAM

that are put into place, typically using DSP methods, FBMC. In an OFDM system, sidelobes widened to either side when carriers were modulated [19]. With a filter bank system, these are taken care of by the filters, leading to a much cleaner carrier. FBMC modulation systems are more intricate than OFDM systems. The IFFT window's longer time domain and lack of abrupt transitions is the primary distinction between OFDM and FBMC. As a result, both its spectral leakage and side lobes in the frequency domain are decreased. The benefits of FBMC include its ability to provide a spectrum-efficient and more selective system, eliminate the need for the cyclic prefix and CP in OFDM, which frees up more room for actual data, and offer reliable narrowband jammers [20].

The OQAM modulation format is the most effective one. Making the signal regeneration possible is the purpose of using OQAM modulation. The OQAM involves creating a half-symbol time shift between the signal's imaginary and real components. The FBMC-OQAM system's initial and final processes are represented by the OQAM system, which is a key component of the system. It confirms the orthogonality of the overlapping adjacent subchannels in the real field. The OQAM pre-processing block creates two new symbols on the transmitter side by confounding among that of every complex-valued QAM character in *di[l]*. So, a production of the $u_i[n]$ was consecutively of a amount which is double once i/p signal $d_i[l]$. that means (n = 2*l*). like publicized in Fig. 3, arrangement for production OQAM symbols trusts on the sub-channel guide [21]. For odd sub-channels for index $2_{\mu-1}, \mu = 1 \dots \frac{M}{2}$ the production o/p could be expressed like.

$$u_{2\mu-1}[2l] = R\{d_{2\mu-1}[l]\}. \quad (5)$$

$$u_{2\mu-1}[2l+1] = j\{d_{2\mu-1}[l]\} \quad (6)$$

Where J{.} and R{.} mean the imaginary and real portions of a quantity character correspondingly. In difference, in the sub-channel through guide $2\mu, \mu = 1 \dots \frac{M}{2}$. the production was specified through.

$$u_{2\mu}[2l] = R\{d_{2\mu}[l]\} \quad (7)$$

$$u_{2\mu}[2l+1] = j\{d_{2\mu}[l]\} \quad (8)$$

The OQAM post-processing was publicized within Fig. 4. the imaginary and real portions of the production of AFB $y_i[n]$ are instead mutual to form the assessed production signal $\hat{d}_l[l]$. like to the OQAM pre-processing. the process is acted upon founded on the sub-channel as.

$$\hat{d}_{2\mu-1}[l] = R\{y_{2\mu-1}[2l]\} + j\{y_{2\mu-1}[2l+1]\} \quad (9)$$

$$\hat{d}_{2\mu}[l] = R\{y_{2\mu}[2l+1]\} + j\{y_{2\mu}[2l]\} \quad (10)$$

Now began to mix the FBMC with the OQAM. when learning the act of FBMC-OQAM scheme it is wanted to understand the basic of this scheme that is the FBMC-QAM [22].

Hermite polynomials $H_n(\cdot)$.represents the core of the prototype filter for FBMC-QAM

$$p(t) = \frac{1}{\sqrt{T_0}} e^{-2\pi\left(\frac{1}{T_0}\right)^2} \sum_{i=\{0,4,8,12\}, 16,20\}} a_i H_i \left(2\sqrt{\pi}\frac{t}{T_0}\right) \quad (11)$$

in which the coefficient could be founded to become

$a_0 = 1.41.$
$a_4 = -3 \times 10^{-3}$.
$a_8 = -8.8 \times 10^{-6}$.
$a_{12} = -2.23 \times 10^{-9}$.
$a_{16} = -4.5 \times 10^{-15}$.
$a_{20} = 1.9 \times 10^{-16}$.

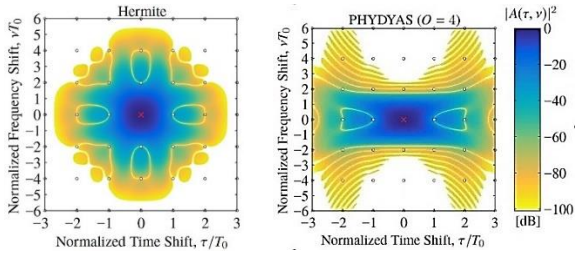

Figure. 5 the prototype filter ambiguity function

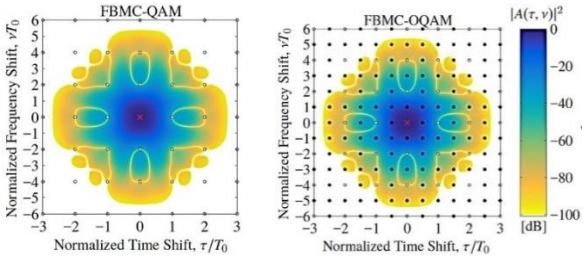

Figure. 6 FBMC-QAM and FBMC-OQAM comparison

that principals to the next possessions that are.

Orthogonal.

$$T = T_0 \ . \ F = \frac{2}{T_0} \ \ this\ lead\ to\ \ TF = two \ .$$

Localization.

$\sigma_t = 0.2015T_0$.

$\sigma_f = \frac{0.403}{T_0}$.

The left portion in Fig. 5 demonstrate the vagueness meaning the

filter of Hermite prototype. Perpendicularity is pragmatic for a period space for $T = T_0$. also, the space of frequency as $F = 2/T_0$. Associated with OFDM, a localize of frequency was greatly improved. the Hermite pulse have the similar form within frequency and time. letting to feat regularities. Also, it is founded on a function of Gaussian and so have a moral combined frequency time localized of $\sigma_t\ \sigma_f = 1.02 \times 1/4\pi$. practically the destined for $\sigma_t\ \sigma_f \geq 1/4\pi$ *equall to* 0.08. creation it comparatively vigorous to channels of the doubly selective [23].

In comparison to standard OFDM with CP and other FBMC techniques, the choice of the FBMC-OQAM scheme was built on a quantity of benefits which made it a extra appealing MCM expertise for upcoming wireless communications. FBMC-OQAM described below.

1. Proposal the filter of prototype with $p(t)$ equal to $p(-t)$ that was orthogonal in space of time. That is $T = T_0$ with a space of frequency. That means $F = 2/T_0$ lead to $TF = 2$.
2. Decrease (orthogonal) frequency-time space with a feature of dual separately. that was, $T = T_0/2$ with $F = 1/T_0$.
3. The phase shift shifts the induced interfering, brought on by the frequency time squeezing to the purely domain of imaginary. $\theta_{l,k} = \pi/2(l+k)$.

Now study the activity of the system in detail to show that performance of this system over other systems. From Fig. 6 it could be shown that FBMC-OQAM has better frequency-time localization than FBMC-QAM.

The FBMC/OQAM scheme is categorized as a disparagingly tasted multi-carrier modulating scheme that operates in a trans-multiplexer conformation with the bank of investigation filter at the handset terminal. and the bank of synthesis filter at the spreader side as its input and output, respectively. Fig. 7 depicts the overall block diagram of a FBMC/OQAM arrangement. the dual primary components of FBMC/OQAM are a filter set scheme and an OQAM post and previous dealing out. In spreader terminal (OQAM preprocessing with SFB), every part of the system (filter-bank and OQAM) is signified by a Fig. 7 (a), Fig. 7b illustrates these two blocks: OQAM post processing and analyses filter-bank (AFB) in the handset terminal. The small amount QAM sign $d_i[l] \in$ C. $i = 0 \cdot \cdot \cdot M - 1$. character directory l was recorded onto $u_i[n] \in$ C via the OQAM preprocessing part. the M was quantity for sub-channels. OQAM sign $u_i[n]$ is multiplex via SFB for generating a higher-rate sign $s[m] \in$ C. the time directory m work $2K$ periods quicker from directory l. where $K = M/2$ was up sampling with down sampling feature using within SFB and AFB correspondingly. rate of K reproduces FBMC/OQAM was a disapprovingly tasted scheme. Instead, the FBMC scheme turn out to be an over-sampled scheme with protector groups when the OQAM system is absent and K > M is used, which results in a reduction in efficiency of spectral. As soon as seeing a perfect canal. the noticed lower-rate sign $\hat{d}_i[l]$ was gotten by de-multiplexing the receiving sign by means of AFB formerly treated via OQAM postprocessing [24].

As exposed in Fig. 7. the combination filter-bank was built of M similar divisions to complex the OQAM signs in $u_i[n]$ via the consistent ith sub-channel. every division for SFB is armed with an up sampler with filter $F_i(z)$. The conveyed sign $s[m]$ was collected through addition SFB production indicator. In receiver sideways. the investigation filter-bank contains of M similar divisions to achieve the double processes SFB. The receiving sign $s[m]$ is primary demultiplexed for consistent sub-bands at that time

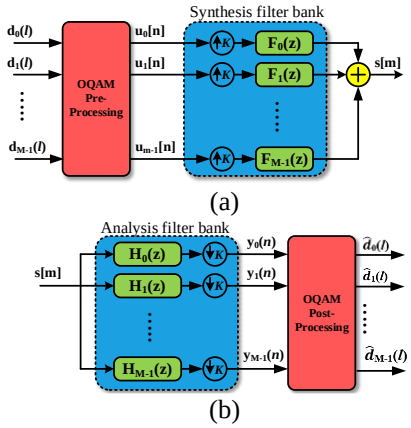

Figure. 7 parts of FBMC/OQAM scheme briefly: (a) transmitting side and (b) receiving side

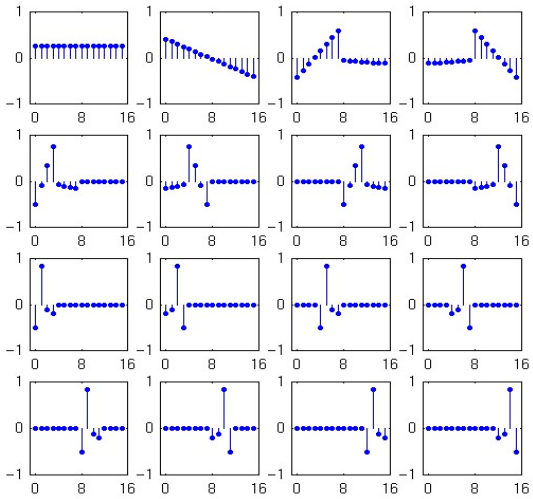

Figure. 8 Slantlet basis (N = 16). the four-scale Slantlet Filter-related bank's 16 x 16 orthogonal matrix vectors

downcast tested via a feature of *K* to produce the o/p signs $y_i[n]$. Together the increase sampling and decrease sampling issues were measured to be the similar rate of *K*=M/2 crossways entirely divisions. The filter-bank scheme splits obtainable channel-bandwidth similarly among the signs for entirely divisions for SFB with AFB. and doing a unchanging FBMC scheme [25].

Now, started researching the Slantlet transform, which is the system's fundamental component. This multi-resolution approach is quite recent and was rely on a discrete wavelet transform (DWT). Actually, it offers superior temporal localization than DWT and was an orthogonal DWT with double zero moments. To reach a discrete temporal basis for an ideal output, the DWT needs a lot of iterations. Instead of repeating the same filter for every level, it uses parallel processing with separate filters set up to every scale. ST filters are rapider than corresponding DWT filters in length. SLT has thus been used to numerous applications and, when compared to other systems, has produced the best results. Because it is never relied on an repeated filter bank. A Slantlet Transform (SLT) is used in this paper. As an alternative, it is built on a structure of bank of filters where various filters were employed for every scale. As a result, the component filter branches have additional degrees of freedom and depend on no particular product form of implementation. Fig. 8 displays the basis for the four-scale filter bank with n=16 [26].

The Daubechies filter, that becomes the bank of filter orthogonal and have K zero moments, is the shortest filter for the two-channel case. The bank of Slantlet filter in K=2 null moments contain filter spans of 8, 4. whereas iterated filter lengths for K=2 null moments are 10, 4. a twice scale repeated Daubechies-2 filter bank's filter distance is therefore dual samples longer than the dual-scale Slantlet filter banks. As more acts are taken, this gap grows wider. every bank of filter offers a multiresolution de-composition and contains a scale expansion feature of 2. Piecewise linear filters are Slantlet filters. Slantlet functions effectively as an iterated DWT filter bank even though it lacks a tree structure. Since ST performs better in communication networks, DWT and SLT have the same computational complexity.

It is helpful to begin by talking about the standard iterated DWT filter bank and a comparable variation, both of which are displayed in Fig. 9. The familiar filters that defined by Daubechies are the smallest filters for the dual-channel scenario where a Filter-bank is orthogonal and contains K null moments. that filters F(z) and H(z) has span four for K=two of null moments. For this system in Fig. 9, the iterated filters are labeled D2 and have lengths of 10 and 4. It is not necessary for the filters to be products in order to construct an orthogonal bank of Filter with k=two of null moments when the filter spans are 8 and 4, as seen in Fig. 9 adjacent to the iterated D2 system. We shall find that the discrepancy increases with the number of stages. There has been a reduction of two samples [27].

The X-axis in Fig. 9 represents the length of the filter while the Y-axis represents the normalized amplitude of the sample.

According to Table 2. It is evident that the Slantlet filter performs better than the D2 filter and produces better results with fewer iterations.

The filters present in the right-hand-side of Fig. 9 are.

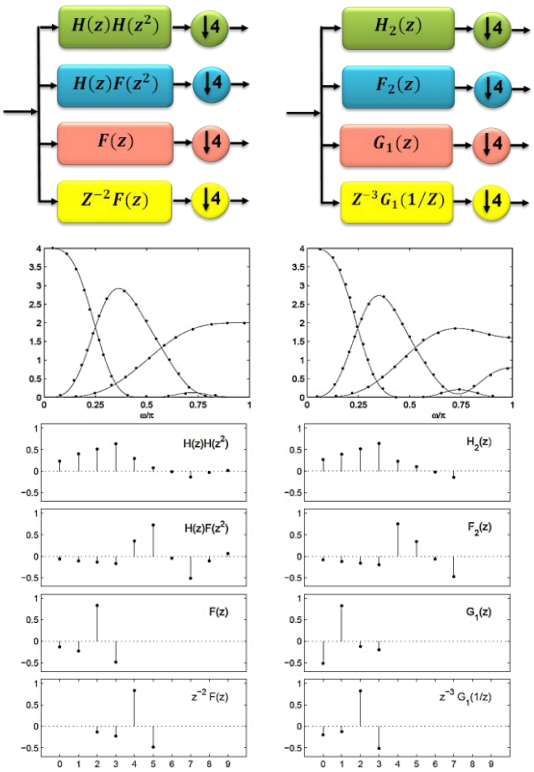

Figure. 9 Comparison of two-scale iterated bank of Slantlet filter vs D2 filter (left-hand side)

Table 2. The D2 and ST Filter banks in comparison

	D_2	**ST**
Support at scale *i*.	3.2^i-2	2^{i+1}
Approximation order.	Two.	Two.
Octave-band.	Run.	Run.
Piecewise linear.	NO.	Run.
Efficient implementation.	Run.	Run.
Orthogonal.	Run.	Run.

$$G_1(z) = \left(-\frac{\sqrt{10}}{20} - \frac{\sqrt{2}}{4}\right) + \left(\frac{3\sqrt{10}}{20} + \frac{\sqrt{2}}{4}\right) z^{-1} + \left(-\frac{3\sqrt{10}}{20} + \frac{\sqrt{2}}{4}\right) z^{-2} + \left(\frac{\sqrt{10}}{20} - \frac{\sqrt{2}}{4}\right) z^{-3} \quad (12)$$

$$F_2(z) = \left(\frac{7\sqrt{5}}{80} - \frac{3\sqrt{55}}{80}\right) + \left(-\frac{\sqrt{5}}{80} - \frac{\sqrt{55}}{80}\right) z^{-1} + \left(-\frac{9\sqrt{5}}{80} + \frac{\sqrt{55}}{80}\right) z^{-2} + \left(-\frac{17\sqrt{5}}{80} + \frac{3\sqrt{55}}{80}\right) z^{-3} + \left(\frac{17\sqrt{5}}{80} + \frac{3\sqrt{55}}{80}\right) z^{-4} + \left(\frac{9\sqrt{5}}{80} + \frac{\sqrt{55}}{80}\right) z^{-5} + \left(\frac{\sqrt{5}}{80} - \frac{\sqrt{55}}{80}\right) z^{-6} + \left(-\frac{7\sqrt{5}}{80} - \frac{3\sqrt{55}}{80}\right) z^{-7} \quad (13)$$

$$H_2(z) = \left(\frac{1}{16} + \frac{\sqrt{11}}{16}\right) + \left(\frac{3}{16} + \frac{\sqrt{11}}{16}\right) z^{-1} + \left(\frac{5}{16} + \frac{\sqrt{11}}{16}\right) z^{-2} + \left(\frac{7}{16} + \frac{\sqrt{11}}{16}\right) z^{-3} + \left(\frac{7}{16} - \frac{\sqrt{11}}{16}\right) z^{-4} + \left(\frac{5}{16} - \frac{\sqrt{11}}{16}\right) z^{-5} + \left(\frac{3}{16} - \frac{\sqrt{11}}{16}\right) z^{-6} + \left(\frac{1}{16} + \frac{\sqrt{11}}{16}\right) z^{-7} \quad (14)$$

It will signify via scale *i*, the scale using which $g_i(n)$ $f_i(n)$, $h_i(n)$ study a signal. The dimension for filter of scale *i* was relative to 2^i . it around true for repeated filter bank. it was precise for ST filter-bank. for overall, the funding of $h_i(n)$ $g_i(n)$ $f_i(n)$, determination be 2^{i+1}.

We must simplify the method in which the Slantlet filter-bank are global for *l* rulers. The scale of *l* bank of filter takes 2*l* in channels. The low-bass filter was entitled $h_l(n)$. The filter together to low-pass filter was named $f_l(n)$. Together $f_l(n)$ with $h_l(n)$ were become trailed by downcast sample by 2^l. A residual 2*l*-2 canals were filtere via $g_i(n)$. it was shift reverse of time to $n = 1, \dots, l-1$. each was trailed by decrease sample by 2^{i+1}. It trails that the filter bank is disapprovingly sampled.

Assume$h_i(n)$ $f_i(n)$ $g_i(n)$ were to each linear in the period $n \in \{0, \dots, 2^i - 1\}$ with the period $n \in \{2^i, \dots, 2^{i+1} - 1\}$. Since in the double aforesaid period the chosen filter. They are stated as and definite by quaternion restrictions.

$$g_i(n). = \begin{cases} a_{0,0} + a_{0,1}n. & for\ n = 0, \dots, 2^i - 1\ . \\ a_{1,0} + a_{1,1}(n - 2^i). & for\ n = 2^i, \dots, 2^{i+1} - 1\ . \end{cases} \quad (15)$$

So, to get $g_i(n)$ that the sought after scale bank of Filter was orthogonal within dual null moments needs gaining constraints "$a_{0,0}$. $a_{0,1}$. $a_{1,0}$.$a_{1,1}$." Therefore, this is resulting [28].
$g_i(n)$ was of unit norm.

$$\sum_{n=0}^{2^{i+1}-1} g_i^2(n) = 1. \quad (16)$$

$g_i(n)$ is orthogonally to its reverse time shifted.

$$\sum_{n=0}^{2^{i+1}-1} g_i(n)\, g_i(2^{i+1} - 1 - n) = 0 \quad (17)$$

$g_i(n)$ annihilates linear discrete time polynomials.

$$\sum_{n=0}^{2^{i+1}-1} g_i(n) = 0\ ,\ \sum_{n=0}^{2^{i+1}-1} n g_i(n) = 0$$

Suppose $m = 2^i$ So.

$$s_1 = 6\sqrt{m/((m^2-1)(4m^2-1))}\ .$$
$$t_1 = 2\sqrt{3/(m.(m^2-1))}\ .$$
$$s_0 = -s_1.(m-1)/2\ .$$
$$t_0 = \left((m+1).s_1/3 - mt_1\right)(m-1)/(2m).$$
$$a_{0,0} = (s_0 + t_0)/2\ .$$
$$a_{1,0} = (s_0 - t_0)/2\ .$$
$$a_{0,1} = (s_1 + t_1)/2\ .$$
$$a_{1,1} = (s_1 - t_1)/2.$$

Thus, the constraints " $a_{0,0}.a_{0,1}.a_{1,0}$. $a_{1,1}$ " Depends on *i*. a similar method run for $f_i(n)$ with $h_i(n)$. the $f_i(n)$ with $h_i(n)$ could be describe in terms of octonary constraints.

$$h_i(n) = \begin{cases} b_{0,0} + b_{0,1}n \ . \quad for\ n = 0, \dots, 2^i - 1. \\ b_{1,0} + b_{1,1}(n - 2^i).\ for\ n = 2^i, \dots, 2^{i+1} - 1. \end{cases} \quad (18)$$

$$f_i(n) = \begin{cases} c_{0,0} + c_{0,1}n. \quad for\ n = 0, \dots, 2^i - 1. \\ c_{1,0} + c_{1,1}(n - 2^i).\ for\ n = 2^i, \dots, 2^{i+1} - 1. \end{cases} \quad (19)$$

The orthogonality and moment circumstances need the subsequent.

1) $h_i(n)$ with $f_i(n)$ are of unit norm.
$\sum_{n=0}^{2^{i+1}-1} h_i^2(n) = one.,\ \sum_{n=zero}^{2^{i+1}-1} f_i^2(n) = one$
2) $h_i(n)$ with $f_i(n)$ are orthogonal to their shifted versions.
$\sum_{n=0}^{2^i-1} h_i\,(n) h_i(n + 2^i) = 0$
$\sum_{n=0}^{2^i-1} f_i\,(n) f_i(n + 2^i) = 0$
$\sum_{n=0}^{2^{i+1}-1} h_i\,(n) f_i(n) = 0$
$\sum_{n=0}^{2^i-1} h_i\,(n) f_i(n + 2^i) = 0$
3) $f_i(n)$ annihilates linear discrete time polynomials.
$\sum_{n=0}^{2^{i+1}-1} f_i\,(n) = 0\ ,\ \sum_{n=0}^{2^{i+1}-1} n\, f_i(n) = 0$
It can be found the next result for $h_i(n)$ with $f_i(n)$ via stating the moment with perpendicularity settings as a multivariate polynomial scheme [29].
Suppose $m = 2^i$.
$u = 1/\sqrt{m}$.
$v = \sqrt{(2m^2 + 1)/3}$.
$b_{0,0} = u.(v + 1)/(2m)$.
$b_{1,0} = u - b_{0,0}$.
$b_{0,1} = u/m$.
$b_{1,1} = -b_{0,1}$.
$q = \sqrt{3/(m.(m^2 - 1))}/m$.
$c_{0,1} = q.(v - m)$.
$c_{1,1} = -q.(v + m)$.
$c_{1,0} = c_{1,1}.(v + 1 - 2m)/2$.
$c_{0,0} = c_{0,1}.(v + 1)/2.$

4. Results and discussion

In this part the many factors will be discussed that will be related with the activity of the proposed structure. These parameters will be PSD, the prototype filter response, power of signal, BER, SIR, and efficiency of the system. For making the comparison of my work in this paper with other works in other papers, the Ref. [30] is chosen for some graphs. The other graphs is made depends on the simulation using the MATLAB package and this is my work in this manuscript.

Table 3. Parameters of the proposed FBMC-OQAM

Parameters	Values
Channel Velocity	100 and 500 Km/h
Channel Power Delay Profile	Vehicular, Flat, AWGN
Channel Doppler Model	Jakes, Uniform
Channel Carrier Frequency	1e9Hz, 5.1e9Hz
OQAM Modulation Order	256, 1024
Prototype Filter	'Hermite, PHYDYAS
Number of Subcarriers	24
Number of Symbols in Time	30
Subcarrier Spacing	15e3 KHz

The parameter that used in simulation was written in Table 3. The first parameter is the PSD. When looking to the Fig. 10 and 11. The low OOB emission was noticed. therefore, the band of guard among dissimilar use situation was comparatively small. OFDM was not suitable for this. Therefore, making filtering and windowing in OFDM. a windowed OFDM system was termed WOLA, UFMC, FOFDM. Though filtering and windowing could really decrease the OOB emission of OFDM. FFT based FBMC still makes improved. when replaced the FFT with the Slantlet transform (proposed system) this led to more performance that means reduce the OOB emission as shown in Fig. 10. In Fig. 11 the two users of 15 and 120 KHz. It is notice that there is interference between two users for all cases except the case of FBMC. The proposed system gives better performance than the system based on FFT.

Now, plots the time and frequency response of different prototype filters that is used in design of FBMC which are: Rectangular, PHYDYAS, Hermite, and RRC in time and frequency. in order to get a better response for filter used in FBMC-OQAM. it must choose the best one which is the Hermite filter as shown in Fig. 12 and 13. Fig. 12 shows the relation between the power and normalize frequency while Fig. 13 represents the relation between power and normalize time. From these two figures it can conclude that Hermite is the best one because it has

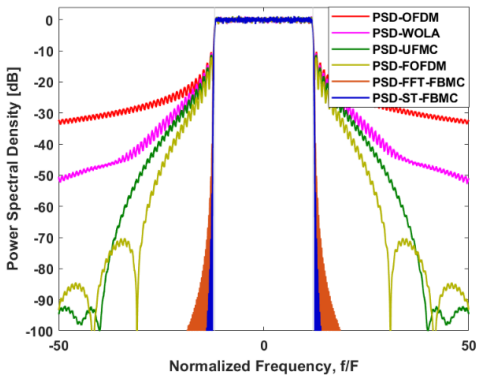

Figure. 10 the relation between PSD with normalized frequency for different systems

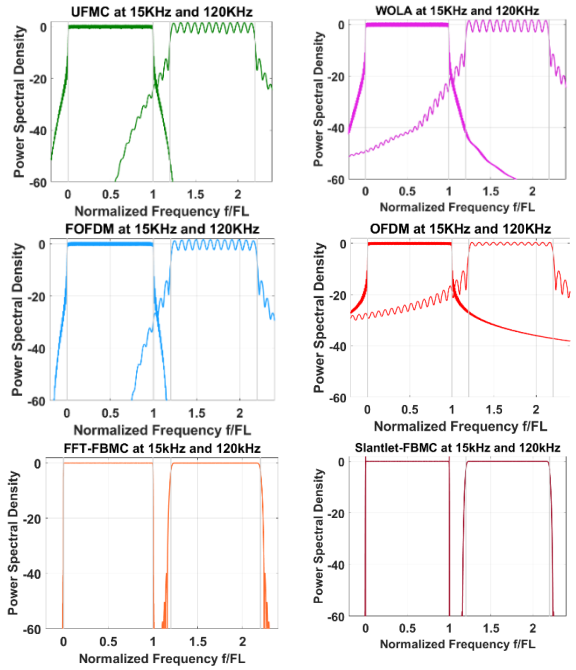

Figure. 11 The relation between PSD and normalized frequency with two users for different systems

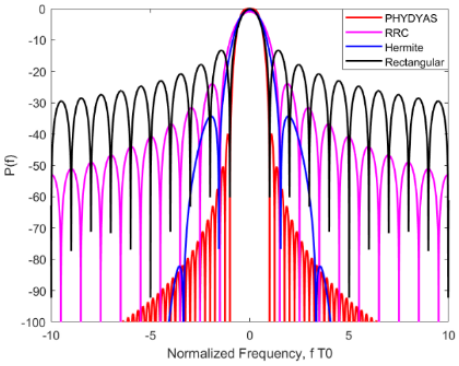

Figure. 12 Frequency response of different prototype filters

the lowest frequency band that means lower OOB emission.

Now the new parameter is the signal power. In Fig. 14 the signal power for the proposed system was

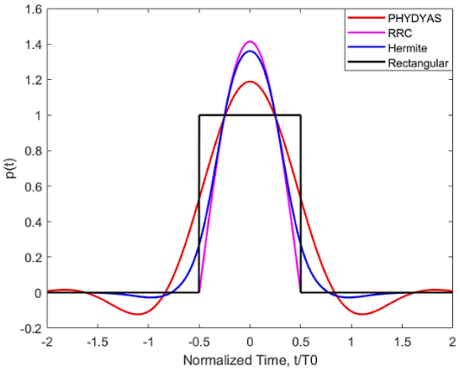

Figure. 13 Time response of different prototype filters

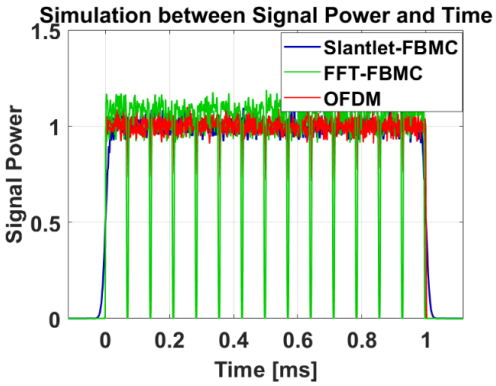

Figure. 14 the relation of signal power with time

still semi fixed along the period in time that means lower PAPR and this is very significant criteria when design the communication scheme.

The next and important parameter is the Bit Error Rate BER. This parameter was calculated by find the relation between BER and signal to noise ratio SNR. More factor was effects on this parameter which will be calculated in order to prove that the proposed system based on Slantlet transform ST-FBMC-OQAM is better than other types of systems. The first factor that will be effect on BER is the speed between sending and receiving end. From Fig. 15 it can be seen that when the speed is low like 100KM/h the three systems are near to other. But when the speed is high (500KM/h) as shown in Fig. 16 then the proposed system was begun to be giving the best performance than other systems.

The second factor that effects on the BER is the frequency of the carrier signal sent between sending and receiving end. It can be concluded from Fig. 17 that when the frequency of the carrier is low like 1GHz the three system provide the small difference in BER. But when the frequency is high as shown in Fig. 18 like 5.1GHz the proposed system gives higher performance with lower BER.

The new factor that will be discussed is the type of modulation which is OQAM. It will be compared between two type of this modulation which are

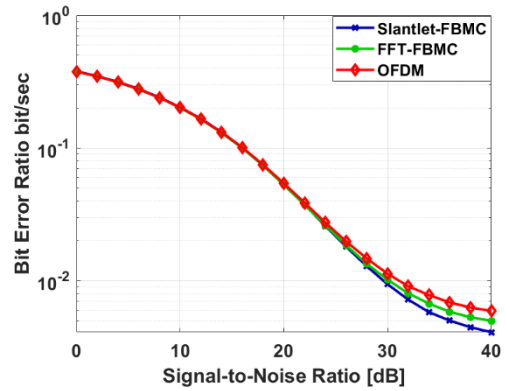

Figure. 15 BER with channel velocity=100Km/h

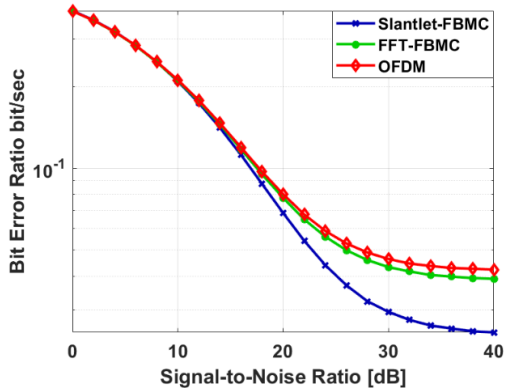

Figure. 16 BER with channel velocity=500Km/h

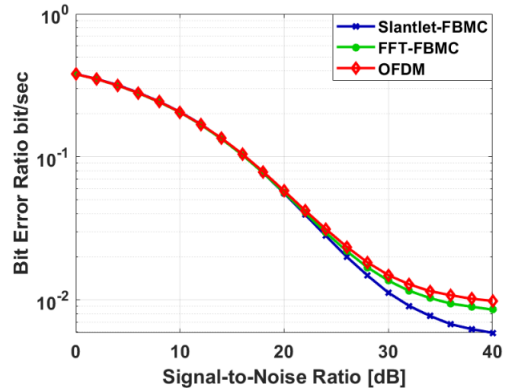

Figure. 17 BER with channel-carrier frequency=1GHz

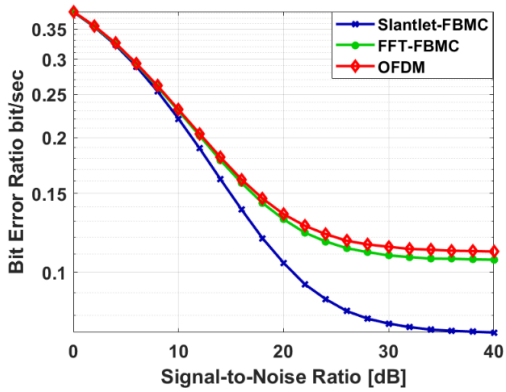

Figure. 18 BER with channel-carrier frequency=5.1 GHz

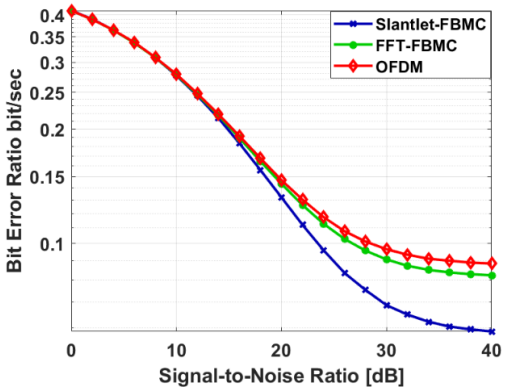

Figure. 19 BER with OQAM-modulation order=256

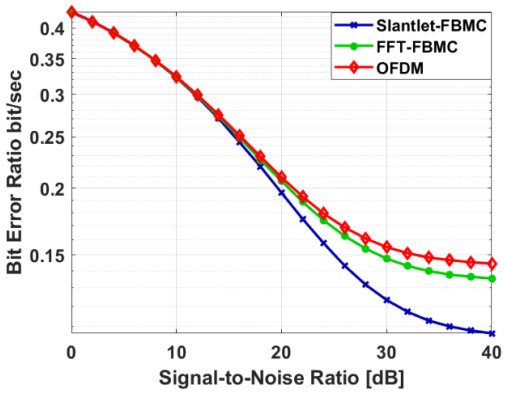

Figure. 20 BER with QAM-modulation order=1024

256OQAM and 1024OQAM. When the level of OQAM is low (256) as shown in Fig. 19 then the system gives lower BER than the system based on 1024OQAM as shown in Fig. 20. But it can be noticed that in two cases the proposed system gives BER lower than other systems.

At this point, the effects of the prototype filter will be discussed. the two types of filters will be taken which are PHYDYAS and Hermite filter. It can be seen that Hermite filter as shown in Fig. 21 gives the best performance than the PHYDYAS filter as shown in Fig. 22. And also, in two cases the proposed system based on Slantlet transform ST gives better performance than other systems.

The next factor effect on the BER is the power delay profile. Taking into account the two types which are Flat and AWGN. At this point it can see the high difference in performance between the two types of power delay profile. as shown in Fig. 23 the AWGN gives better performance that in Flat delay profile shown in Fig. 24. Also, the proposed system in two cases gives the high performance than other two system.

The last factor that effects on the BER is the channel doppler model. Taking the two models which are Jakes and Uniform model. It can be seen from Fig. 25 that the Jakes model gives the better performance

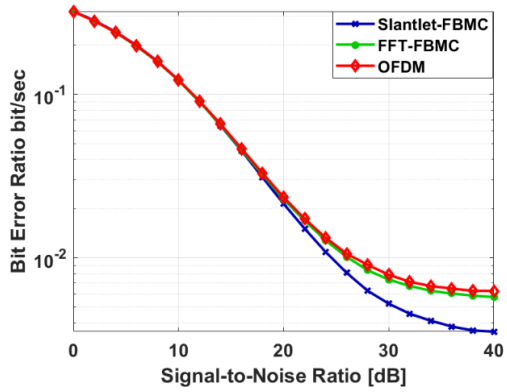

Figure. 21 BER with prototype filter is Hermite

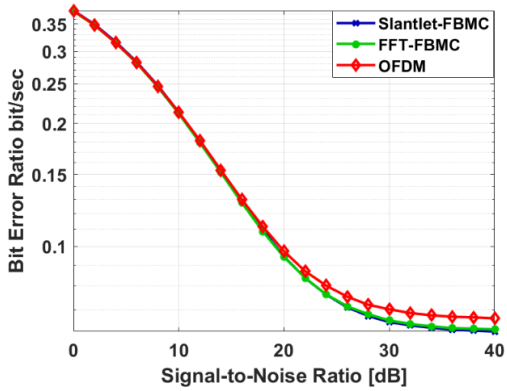

Figure. 22 BER with prototype filter is PHYDYAS

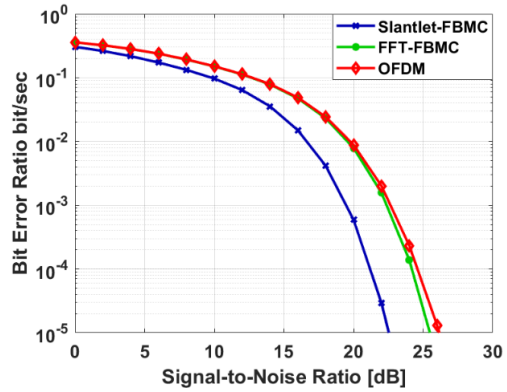

Figure. 23 BER with power delay profile is AWGN

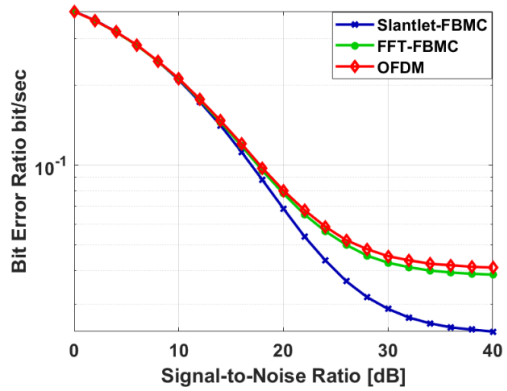

Figure. 24 BER with power delay profile is flat

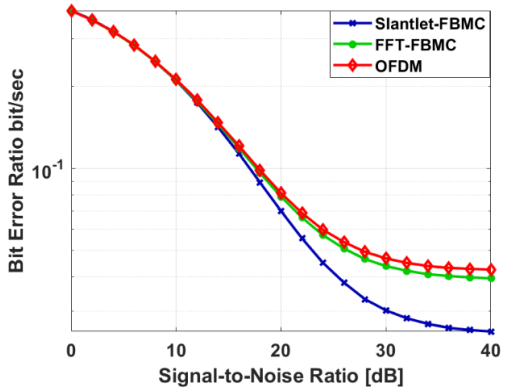

Figure. 25 BER with channel doppler model is jakes

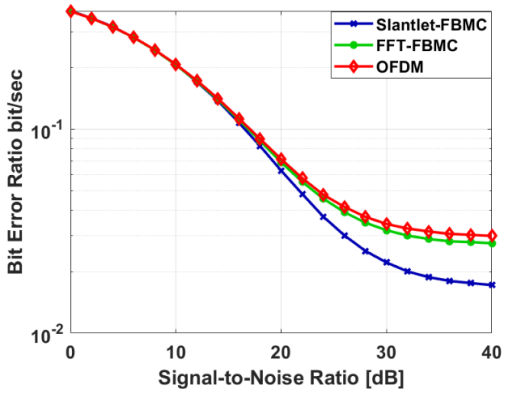

Figure. 26 BER with channel doppler model is uniform

than Uniform model shown in Fig. 26. The proposed model based on Slantlet transform gives the higher performance than other system when gives lower BER.

Now, talking about the new parameter which is SIR. Also, there are two factors will affect the performance of the system depending on SIR. The first one is the type of the filter which is PHYDYAS and Hermite filter. It can notice that Hermite filter as shown in Fig. 27 gives better performance than another filter which is the PHYDYAS filter as shown in Fig. 28.

The next factor that effects on the SIR parameter is the overlap factor which will take as 2 and 4. It can be notice that when increase the overlap factor to 4 as shown in Fig. 29 the performance will be improved and gives better than the system with overlap equal to 2 as shown in Fig. 30. Also, the proposed system was overcome the other system when comparing with it. when find the relation between SIR and frequency offset. it could achieve a new scheme gives the better performance than other system as shown in Fig. 31. Finally, the last parameter that effect on the proposed system is the relation between the efficiency with the number of subcarriers. From Fig. 32 it is shown that the new scheme gives the high efficiency when comparing with the other systems.

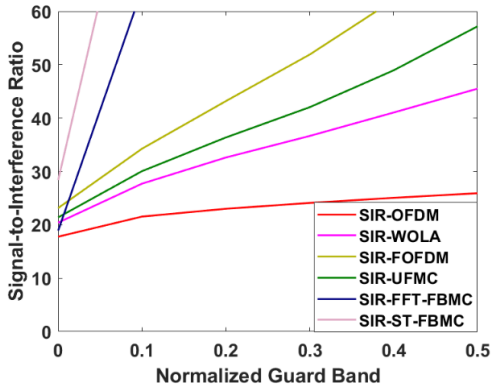

Figure. 27 SIR with filter is Hermite

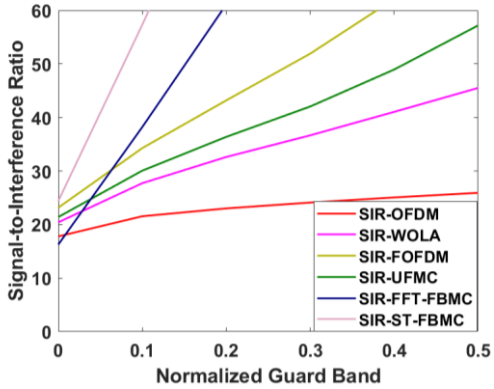

Figure. 28 SIR with filter is PHYDYAS

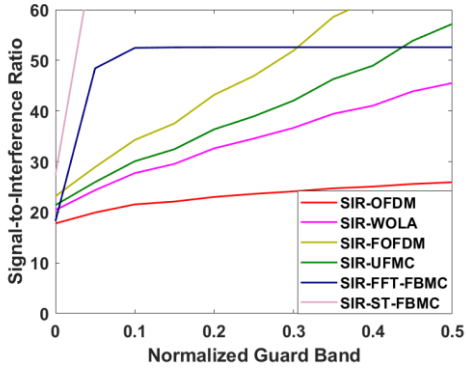

Figure. 29 SIR with overlap factor is 4

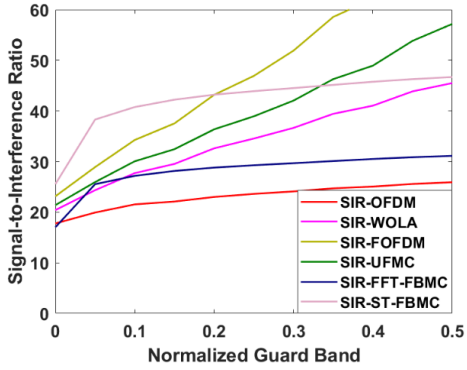

Figure. 30 SIR with overlap factor is 2

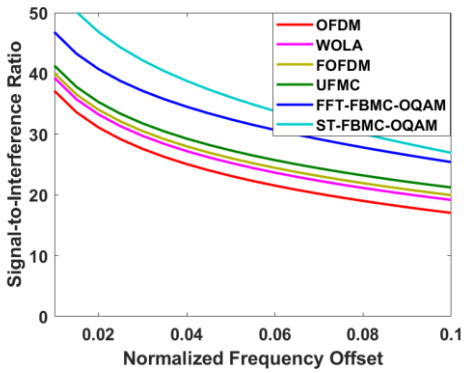

Figure. 31 Relation between SIR with normalize frequency offset

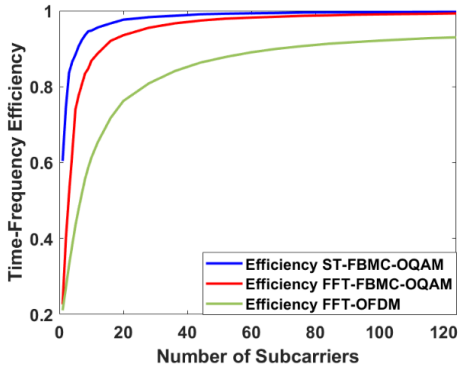

Figure. 32 relation between efficiency with no. of subcarrier

5. Conclusion

The new combination of FBMC-OQAM based on the Slantlet Transform ST was done. Also, the other system like WOLA, UFMC, FOFDM, and FFT based FBMC-OQAM were designed using the MATLAB backage in order to compare these systems with the new one. This new system was tested under more than one parameter in order to prove that this system was overcome the other systems. these parameters were different in his effect on the system. In the first must mention the OOB activity as shown in figures 10 and 11. From these two figures the new system gives lower OOB as compare with other system. The second one is the type of filter used.

According to figures 12 and 13 which represents the relation between normalize frequency and time with power. The Hermite filter gives high activity with lower vibration. So, Hermite filter will be chosen. Along the time the signal power for the proposed system as shown in figure 14 gives lower vibration and this gives lower PAPR and then lower drop of power. Figures 15 and 26 gives the fact that this system gives high activity with lower BER in high speed, high frequency, high modulation order, high active prototype filter which is Hermite, high Power delay profile, high Channel Doppler Model.

All these parameters are needed in 5G communication system.

The other important factor is the SIR. A greater Signal-to-Interference Ratio (SIR) signifies enhanced signal quality, as it implies that the desired signal holds greater strength compared to interference or noise. Consequently, this facilitates more accurate interpretation and decoding of transmitted information by the receiver. Conversely, a lower SIR implies diminished signal quality, as the interference or noise becomes more prominent in relation to the desired signal. in this factor the circumstances were effects on this factor such as filter type, overlap factor, and frequency offset as shown in figures 27 to 31. In all these factors the proposed system gives SIR higher than other system in all cases.

The final parameter used in this simulation was the efficiency and its relation with the number of subcarriers as shown in figure 32. It can be notice that the new system gives efficiency higher than other system based on FFT. From all these figures it can conclude that the proposed system gives higher activity than other system and more suitable for using in 5G or higher communication systems.

Conflicts of interest

The author declared that no conflict of interest for that manuscript.

Author contributions

A contribution of writer for that manuscript can be briefly describe as the author wrote the paper with all related arrangements. Also, complete all the software requirements for this paper and responsible for extracting the graphs, tables and figures for this paper. the author had approved the final version.

Acknowledgments

The author wishes to extend sincere thanks for the unlimited moral support from the Middle Technical University-Iraq and in particular for the Technical Institute-Kut throughout the period of completion of the research.

References

[1] T. Ihalainen, A. Ikhlef, J. Louveaux, and M. Renfors, "Channel equalization for multi-antenna FBMC/OQAM receivers", *IEEE Transaction on Vehicular Technology*, Vol. 60, No. 5, pp. 2070-2085, 2011.

[2] H. M. A. Abbas, R. F. Chisab, and M. J. Mnati, "Monitoring and controlling the speed and direction of a DC motor through FPGA and comparison of FPGA for speed and performance optimization", *International Journal of Electrical and Computer Engineering*, Vol. 11, No. 5, pp. 3903-3912, 2021.

[3] N. S. Kim, "Link Balance and Performance of UAM in NOMA-based Cellular Networks", *International Journal of Intelligent Engineering and Systems*, Vol. 15, No. 1, pp. 490-498, 2022, doi: 10.22266/ijies2022.0228.44.

[4] K. R. Gajulapalli and M. S. Gnanadhas, "Analysis of PAPR and BER Reduction in MIMO-OFDM using Hybrid Moth Flame-Improved Firefly Algorithm", *International Journal of Intelligent Engineering and Systems*, Vol. 15, No. 4, pp. 97-105, 2022, doi: 10.22266/ijies2022.0831.10.

[5] A. Lalitha and G. H. Reddy, "Blind Channel Estimation Using Enhanced Independent Component Analysis for MIMO-OFDM System", *International Journal of Intelligent Engineering and Systems*, Vol. 15, No. 5, pp. 25-34, 2022, doi: 10.22266/ijies2022.1031.03.

[6] A. S. Hameed and D. T. A. Zuhairi, "A Multi-level Compression Scheme for Peak to Average Power Ratio Mitigation in SC-FDMA Communication System", *International Journal of Intelligent Engineering and Systems*, Vol. 15, No. 5, pp. 103-112, 2022, doi: 10.22266/ijies2022.1031.10.

[7] M. T. Ali, Y. R. Muhsen, R. F. Chisab, and S. N. Abed, "Evaluation Study of Radio Frequency Radiation Effects from Cell Phone Towers on Human Health", *Radioelectronics and Communications Systems*, Vol. 64, No. 3, pp. 155-164, 2021.

[8] A. Azeez and S. Tarannum, "Prime Learning Ant Lion Optimization with Precoding and Companding for PAPR Reduction in MIMO-OFDM", *International Journal of Intelligent Engineering and Systems*, Vol. 15, No. 5, pp. 439-449, 2022, doi: 10.22266/ijies2022.1031.38.

[9] M. J. Ameen and S. S. Hreshee, "Securing Physical Layer of 5G Wireless Network System over GFDM Using Linear Precoding Algorithm for Massive MIMO and Hyperchaotic QR-Decomposition", *International Journal of Intelligent Engineering and Systems*, Vol. 15, No. 5, pp. 579-591, 2022, doi: 10.22266/ijies2022.1031.50.

[10] H. S. Hamid and R. F. Chisab, "The calculation of the field of an antenna located near the human head", *Bulletin of Electrical Engineering and Informatics*, Vol. 10, No. 6, pp. 3282-3288, 2021.

[11] G. Matz, H. Bolcskei, and F. Hlawatsch, "Time-frequency foundations of communications:

Concepts and tools", *IEEE Signal Processing Magazine*, Vol. 30, No. 6, pp. 87-96, 2013.

[12] B. K. Mohammed, R. F. Chisab, and A. H. Alwaily, "The Powerful Method for Smart Classroom Communication Rely on IoT", In: *Proc. of International Conf. On Advance of Sustainable Engineering and its Application (ICASEA)*, Wasit, Iraq, pp. 33-36, 2021.

[13] V. G. Tikka and R. Sivashanmugam, "Error Correction Using Hybrid Coding Algorithm for BER Reduction in MIMOOFDM", *International Journal of Intelligent Engineering and Systems*, Vol. 15, No. 6, pp. 618-628, 2022, doi: 10.22266/ijies2022.1231.55.

[14] A. K. H. A. Ali and F. S. Hasan, "High Level Security of Image Transmission through STBC-COFDM System", *International Journal of Intelligent Engineering and Systems*, Vol. 16, No. 1, pp. 154-162, 2023, doi: 10.22266/ijies2023.0228.14.

[15] R. Hidayat, A. F. Isnawati, and B. Setiyanto, "Channel Estimation in MIMO-OFDM Spatial Multiplexing Using Least Square Method", In: *Proc. of International Symp. on Intelligent Signal Processing and Communication Systems (lSPACS)*, Chiang Mai, Thailand, 2017.

[16] M. Payar´o, A. P. Iserte, and M. N´ajar, "Performance comparison between FBMC and OFDM in MIMO systems under channel uncertainty", In: *Proc. of the European Wireless Conf. (EW)*, Lucca, Italy, pp. 1023-1030, 2010.

[17] R. Zakaria and D. L. Ruyet, "A novel filter-bank multicarrier scheme to mitigate the intrinsic interference: application to MIMO systems", *IEEE Transactions on Wireless Communications*, Vol. 11, No. 3, pp. 1112-1123, 2012.

[18] S. V. Reddy and C. S. Kumar, "An Excavated PSO-SQP Mechanisms for an Effective Radar Transmission in MIMO-OFDM Communication Systems", *International Journal of Intelligent Engineering and Systems*, Vol. 16, No. 1, pp. 163-172, 2023, doi: 10.22266/ijies2023.0228.15.

[19] P. Kansal and A. K. Shankhwar, "FBMC vs OFDM Waveform Contenders for 5G Wireless Communication System", *Wireless Engineering Technology*, Vol. 8, No. 4, pp. 59-70, 2017.

[20] E. Kofidis and A. Rontogiannis, "Adaptive BLAST decision-feedback equalizer for MIMO-FBMC/OQAM systems", In: *Proc. of International Symp. on the Personal Indoor and Mobile Radio Communications, PIRMC*, Istanbul, Turkey, pp. 841-846, 2010.

[21] M. E. Tabach, J. Javaudin, and M. H`elard, "Spatial data multiplexing over OFDM/OQAM modulations", In: *Proc. of International Conf. On Communications*, Glasgow, Scotland, pp. 4201-4206, 2007.

[22] M. Caus and A. P. Neira, "Transmitter-receiver designs for highly frequency selective channels in MIMO FBMC systems", *IEEE Transactions on Signal Processing*, Vol. 60, No. 12, pp. 6519-6532, 2012.

[23] X. Yang, S. Yan, X. Li, and F. Li, "A Unified Spectrum Formulation for OFDM, FBMC, and F-OFDM", *Electronics*, Vol. 9, No. 8, pp. 1-15, 2020.

[24] G. Kongara, C. He, L. Yang, and J. Armstrong, "A Comparison of CP-OFDM, PCC-OFDM and UFMC for 5G Uplink Communications", *IEEE Access*, Vol. 7, pp. 157574-157594, 2019.

[25] R. Nissel and M. Rupp, "OFDM and FBMC-OQAM in doubly selective channels: Calculating the bit error probability", *IEEE Communication Letter*, Vol. 21, No. 6, pp. 1297-1300, 2017.

[26] W. Selesnick, "The Slantlet transform", *IEEE Transactions on Signal Processing*, Vol. 47, No. 5, pp. 1304-1313, 1999.

[27] P. C. Mali, B. B. Chaudhuri, and D. D. Majumder, "Some properties and fast algorithms of slant transform in image processing", *Signal Processing*, Vol. 9, No. 4, pp. 233-244, 1985.

[28] G. Panda and S. K. Meher, "An Efficient Approach to Signal Compression using Slantlet Transform", *IETE Journal of Research*, Vol. 46, No. 5, pp. 299-307, 2000.

[29] R. T. Mohammed and B. E. Khoo, "Image Watermarking Using Slantlet Transform", In: *Proc. of International Symp. on Industrial Electronics and Applications (ISIEA)*, Bandung, Indonesia, pp. 281-286, 2012.

[30] R. Nissel, S. Schwarz, and M. Rupp, "Filter Bank Multicarrier Modulation Schemes for Future Mobile Communications", *IEEE Journal on Selected Areas in Communications*, Vol. 35, No. 8, pp. 1768-1782, 2017.